Analysis of Thermal Control Characteristics of VCHP by the Charging Mass of Non-Condensible Gas

Jeong-Se Suh†, Young-Sik Park*, Kyung-Taek Chung, Byoung-Gi Kim

School of Mechanical & Aerospace Engineering, GyeongSang National University, ReCAPT, Jinju 660-701, Korea

**Department of Car-Electronics, Korea Polytechnic Ⅶ College, Changwon 641-772, Korea*

Key words: Variable conductance heat pipe, Non-condensible gas, Mass fraction, Mesh wick, Thermal control

ABSTRACT: This study has been performed to investigate the thermal performance of variable conductance heat pipe (VCHP) with screen meshed wick. The active length of condenser section in a VCHP is varied by non-condensible gas, which controls the operating temperature, and the heat capacity of VCHP is controlled by the operating temperature. In this study, numerical analysis of the VCHP based on the diffusion model of non-condensible gas is done for the thermal control performance of VCHP. Water is used as a working fluid and nitrogen as a control non-condensible gas in the copper tube. As a result, the thermal conductance of VCHP has been compared with that of constant conductance heat pipe (CCHP) corresponding to the variation of operating temperature.

Nomenclature

A_V : vapor core cross-sectional area [m^2]
D : diffusion coefficient [m^2/s]
$h_{f,c}$: interface heat transfer coefficient between heat pipe and heat sink at condenser [$W/m^2 \cdot K$]
k_e : effective thermal conductivity of liquid-saturated wick [$W/m^2 \cdot K$]
k_p : thermal conductivity of pipe material [$W/m^2 \cdot K$]
M_g : gas molecular weight
M_v : vapor molecular weight
$\dot{m}_g$: gas mass flow rate [kg/s]
$\dot{m}_v$: vapor mass flow rate [kg/s]
P_v : vapor pressure [Pa]
R_g : gas constant [N·m/kg·K]
r_i : inside radius of pipe [m]
r_o : outside radius of pipe [m]
r_v : vapor core radius [m]
T_{opr} : operating temperature [K]
T_p : wall temperature of pipe [K]
T_s : heat sink temperature [K]
x_g : length of the condenser [m]

Greek symbols

ρ : sum of the vapor and gas density [kg/m^3]

† *Corresponding author*
Tel.: +82-55-751-5312; fax: +82-55-757-5622
E-mail address: jssuh@gnu.ac.kr

1. Introduction

Of the various methods of transporting heat, the heat pipe is one of the most efficient device known today. The heat pipe was first conceived by Gaugler of the General Motors Corporation in the U.S.[1] In a conventional heat pipe, the operating temperature is determined by the heat source and heat sink conditions.

Thus, a change in the input heat load or

evaporator temperature will cause a change in the condenser temperature, although the condenser (or evaporator) temperature needs to be held constant with a variable input heat load. Because of its nearly constant conductance, the conventional heat pipe is incapable of these types of temperature control. The variable conductance heat pipe (VCHP) is therefore designed for the constant condenser (or evaporator) temperature independent of the variable thermal load. Several techniques have been used to moderate the change in the operating temperature in response to the changes in the operating conditions by varying the total thermal conductance of the heat pipe.

As the thermal load at the heat source is increased, the vapor pressure in the active portion of the pipe rises and consequently compresses the non-condensible gas and increases the active length of the condenser. The increased active length of the condenser results in reducing the thermal resistance of heat pipe.

A survey of literatures reveals that Marcus[2] developed the model that analyzes the heat transport behavior of VCHP, and Chi[3] presented the modified model of VCHP in a steady-state operation. Bobco[4] has analyzed the thermal performance of VCHP from one-dimensional diffusion model, and the maximum heat transport capacity of VCHP. Kobayashi et al.[5] and Sauciuc et al.[6] studied analytically the thermal performance of thermosyphon with non-condensible gas reservoir. Peterson[7] studied the phenomena of convection and diffusion of vapor and non-condensible gas in a reservoir.

Park et al.[8] studied numerical evaluation for gas-loaded VCHP which has been based on one-dimensional diffusion model considering the diffusive expansion of non-condensible gas due to the gradient of gas concentration at the interface between vapor and gas.

2. Analysis

2.1 Basic equation

For one-dimensional steady diffusion models, the non-condensible gas is assumed to be stationary in the inactive condenser section and the heat pipe is assumed to be at steady-state conditions. The concentration distribution of gas at the vapor-gas interface can be determined from the Fick's law for binary mixture mass diffusion.

An elementary control volume in the pipe wall of the condenser section of a gas-loaded heat pipe is shown in Fig. 1. The heat conduction in the vapor is assumed to be neglected and constant physical properties are assumed, and no radial variations of temperature

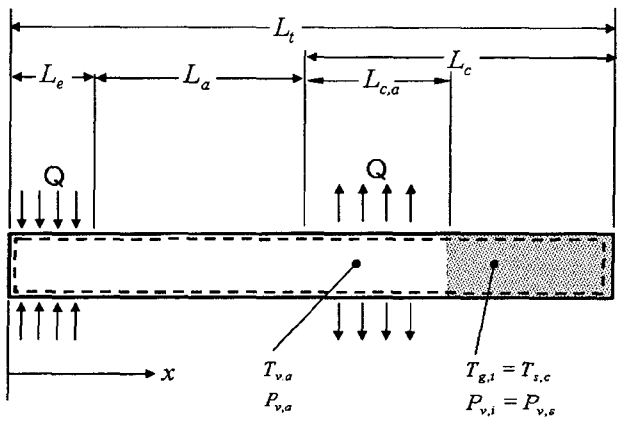

Fig. 1 Schematic diagram of variable conductance heat pipe without gas reservoir.

and mass concentration in the vapor, wall, and wick are assumed. Additional assumptions are given that the mass fraction of the non-condensible gas is zero at the beginning of condenser section, the liquid-vapor interface temperature is equal to the saturation vapor temperature at the partial vapor pressure and the heat pipe operated in the steady-state with the non-condensible gas stationary. Conservation of energy in the pipe wall is calculated by the following equation:

$$\frac{d}{dx}\left[k_p\pi(r_o^2-r_i^2)\frac{dT}{dx}\right]+\frac{2\pi r_i k_e}{r_i-r_v}(T_{wv}-T_p) - 2\pi r_o h_{f,c}(T_p-T_s)=0 \quad (1)$$

Considering the mass flow rate of the gas though interface, both the conservations of convection and mass diffusion yield.

$$\dot{m}_g=\chi_g(\dot{m}_v+\dot{m}_g)-A_v\rho D\frac{d\chi_g}{dx} \quad (2)$$

Since the non-condensible gas of condenser is assumed stationary, $\dot{m}_g=0$, Eq. (2) can be written as

$$\dot{m}_v=A_v\rho D\frac{d\ln\chi_g}{dx} \quad (3)$$

Conservation of energy requires that all the latent heat released by the condensation process be conducted into the liquid saturated wick.

$$\frac{d\dot{m}_v}{dx}=-\frac{2\pi r_i k_e}{\lambda(r_i-r_v)}(T_{wv}-T_p) \quad (4)$$

Equations (1)~(4) describe the mass flow behavior of the gas-loaded heat pipe, assuming one-dimensional mass diffusion. The saturation vapor temperature at the liquid-vapor interface can be related to the mass fraction and vapor pressure from the Clausis-Clapeyron saturation relationship with the vapor pressure upstream into the vapor-gas mass diffusion region.

$$T_{wv}=f(P_v') \quad (5)$$

$$P_v'=\frac{M_g(1-\chi_g)P_v}{M_v\chi_g+M_g(1-\chi_g)} \quad (6)$$

The vapor pressure upstream results in a decrease of the interface temperature as the mass fraction increases. For this model, the total pressure in the active condenser section is equal to the partial vapor pressure since non-condensible gas is assumed to be absent. The ρ is the sum of the vapor and gas densities as follows:

$$\rho=\rho_v(T_{wv})+\frac{M_v\chi_g P_v}{R_g T_{wv}[\chi_g M_v+M_g(1-\chi_g)]} \quad (7)$$

Boundary conditions at the end of condenser required to these equations are given as

$$x_g=0 \qquad (x=L_c) \quad (8)$$

$$T_{wv}=T_v \qquad (x=L_c) \quad (9)$$

At the condenser end cap, the axial gradients of the temperature and vapor mass flow rate sets to be zero due to adiabatic and impermeable condition.

$$\frac{dT_p}{dx}=0 \qquad (x=L_t) \quad (10)$$

$$\dot{m}_v=0 \qquad (x=L_t) \quad (11)$$

2.2 Numerical method for established problem

The specification of heat pipes used in this study are as follows: total length is 500 mm, outside diameter 12.7 mm, inside diameter 11.1 mm copper tube with inserted copper screen mesh wick.

Other specifications of VCHP are shown in Table 1. The container material of VCHP is copper. The heat pipe is charged with a distilled water as working fluid and nitrogen as non-condensible gas. Water is known as low-cost,

Table 1 Specification of variable conductance heat pipe used in this study

Description	Specification
Screen mesh number	#200, 1 Layer
Total length	0.5 m
Evaporator length	0.1 m
Adiabatic length	0.05 m
Condenser length	0.35 m
Pipe diameter (O.D)	1.27×10^{-2} m
Pipe diameter (I.D)	1.11×10^{-2} m
Inclination angle	90° ~ −5°
Cooling water	276 ~ 303 K

non-poisonous, high latent heat material and having good compatibility with copper. The distilled water is charged by 4.8 g corresponding to 40% of evaporator volume of heat pipe. The non condensable gas is also charged by 1.0×10^{-6} kg in HP1, 3.4×10^{-6} kg in HP2 and 5.0×10^{-6} kg in HP3, respectively. HP4 is a constant conductance heat pipe (CCHP) in which heat transfer resistance is conventionally not varied for the increasing heat load. The heat pipe used in this study is screen mesh type VCHP without a gas reservoir. The operating temperature of heat pipe can be usually defined by the mean temperature of adiabatic section during the heat pipe operation.

In Eqs. (1) ~ (4), all equations have to be solved simultaneously for T, χ_g and $\dot{m}$, using numerical method of Runge-Kutta.

The heat transfer coefficient in the condenser section with water cooling is considered 690 $W/m^2\cdot K$. The numerical results from the above equations are obtained by varying quantity of non-condensible gas and by varying of operating temperature, respectively.

3. Results and discussion

3.1 Distribution of mass fraction and pressure

Figure 2 shows the axial distribution of mass fraction of NCG for several amounts of non-condensible gas at cooling water temperature 293 K, heat input 130 W and a vertical mode of heat pipe.

Mass fraction of gas for HP1, which has the least charging mass of non-condensible gas, is 0.82 at the axial position of 0.36 m. Mass fraction and interface position of HP2 are 0.91 and 0.28 m, respectively. Mass fraction of HP3, which has the largest charging amount of non-condensible gas is 0.93. In case of high NCG mass, the mass fraction of NCG increases with gas density, and consequently the active length of condenser decreases.

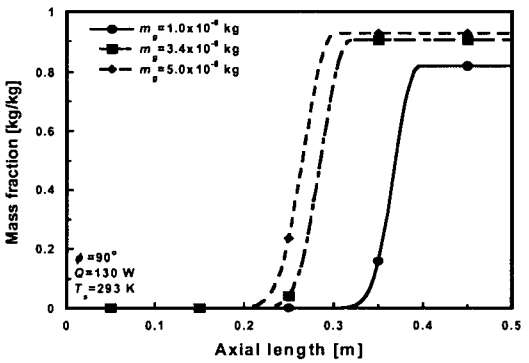

Fig. 2 Axial distribution of mass fraction with the mass of NCG.

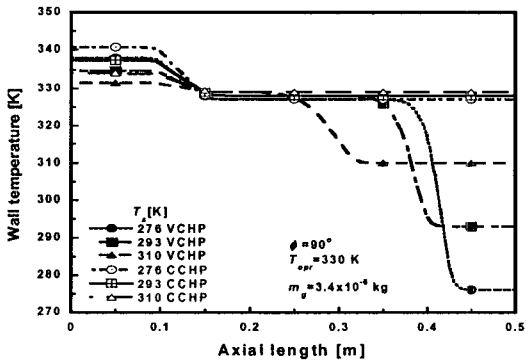

Fig. 3 Distribution of wall temperature with the ambient temperature of condenser of VCHP.

3.2 Effect of cooling water temperature

Figure 3 shows the axial variation of wall temperature of HP2 and HP4 heat pipe with temperature of cooling water changed at the fixed operating temperature of 330 K and a vertical mode. When the cooling water temperature maintains 293 K, the average temperatures of evaporator of VCHP and CCHP are 337.3 K and 334.7 K, respectively. The evaporator temperature of VCHP is consequently 2.6 K higher than that of CCHP. These phenomena mean that the VCHP releases heat less than CCHP due to the increasing inactive length of condenser section of VCHP.

3.3 Effect of charged non-condensible gas mass

Figure 4 demonstrates the pipe wall temperature distribution. The cooling water temperature is 293 K and heat input is 130 W. The interface of HP3 having a large quantity of non-condensible gas was located in 0.26 m at 335.8 K operating temperature, 0.28 m for HP2 at operating temperature of 330.1 K and 0.36 m for HP1 at operating temperature of 309.1 K, respectively. As is observed in Fig. 4, the effect of heat rejection of HP4 (CCHP) is much higher at operating temperature of 309.1 K than that of VCHP, as the total condenser section of heat pipe is active.

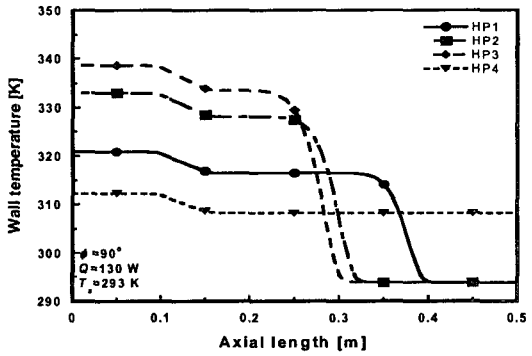

Fig. 4 Axial variation of wall temperature with mass of NCG at 130 W.

3.4 Effect of inclination angle of heat pipe

Figure 5 shows the variation of capillary limit on heat transfer rate with operating temperature for 7 steps of inclination angle. At initial temperature of 326.8 K, the capillary limit on heat transfer rate is 126.5 W for inclination angle of 90°, 111.6 W for 60°, 105.4 W for 45°, and 103.5 W for 30°, respectively. At the horizontal position (the inclination angle is 0°), the capillary limit on heat transfer rate is 9.4 W. Top heating mode of heat pipe for all operating temperature studied in this work causes it to be dry-out. These phenomena mean that the heat pipe operates well due to the gravity effects in a vertical position. For horizontal and

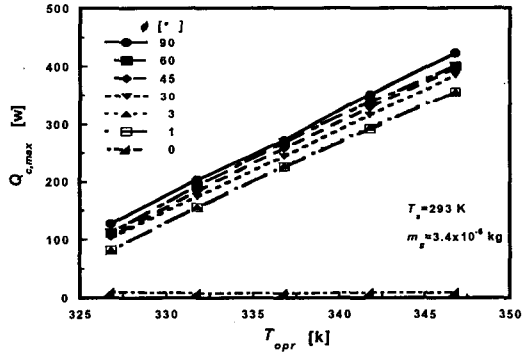

Fig. 5 Distribution of capillary limit on heat transfer rate with inclination angle for HP2.

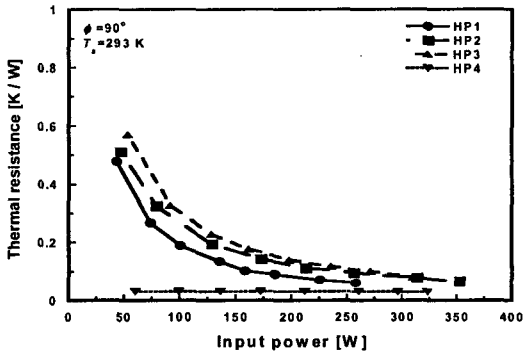

Fig. 6 Distribution of thermal resistance with the input power of VCHP and CCHP.

top heating mode, VCHP happens to be dry out with inclination angle reduction due to the poor returning of working fluid to the evaporator of heat pipe.

3.5 Thermal resistance

Figure 6 shows the distribution of thermal resistance with input power imposed on the VCHP and CCHP. In case of CCHP, when the input power is 60.6 W and 323.3 W, the thermal resistance is 0.0295 K/W and 0.028 K/W, respectively. In spite of large variation of input power, the thermal resistance of CCHP is found constant. But for VCHP, it is clear that the thermal resistance proportionally increases with the amount of non-condensible gas increase. These phenomena result from the increasing inactive zone of condenser with NCG charging mass increasing at the same input power. This situation causes both thermal resistance and operating temperature to increase.

4. Conclusions

The results from VCHP thermal performance analysis with diffusion effect model can be summarized as follows:

(1) An increase in the operating temperature causes high vapor pressure, and consequently gas moves to the end of condenser. An increasing mass of non-condensible gas causes the active condenser zone to decrease and the wall temperature of heat pipe thus increases.

(2) For VCHP, the thermal resistance can be controlled by non-condensible gas with the heat input increase and the variation of operating temperature can be lower than that of CCHP.

(3) The effect of condenser cooling water showed that the temperature difference between evaporator and condenser of VCHP is smaller than that of CCHP.

(4) As the inclination angle of heat pipe is decreased from vertical to horizontal, the operating temperature is proportionally increased.

Acknowledgements

This work is partially supported by Nuri, the 2nd stage BK21 Project, and ERI.

References

1. Gaugler, K. S., 1942, Heat Transfer Device. US patent. 2350348 April. 21 Dec. Published 6 June, 1944.
2. Marcus, B. D., 1971, Theory and design of variable conductance heat pipe: Control techniques, 2nd report by TRW Inc. to NASA, Contact No. NAS2-5503.
3. Chi, S. W., 1976, Heat Pipe Theory and Practice, McGraw-Hill, New York.
4. Bobco, R. P., 1989, Variable conductance heat pipe performance analysis, Journal of Thermophysics, Vol. 3, No. 1, pp. 33-41.
5. Kobayashi, Y., Okumura, A. and Matsue, T., 1991, Effect of gravity and non condensable gas levels on condensation in variable conductance heat pipe, Journal of Thermophysics, Vol. 5, Vo. 1, pp. 61-68.
6. Sauciuc, I., Akbarzadeh, A. and Johnson, P., 1996, Temperature control using variable conductance closed two-phase heat pipe, Heat Mass Transfer, Vol. 23, No. 3, pp. 427-433.
7. Peterson, P. F. and Tien, C. L., 1990, Mixed double-diffusive convection in gas-loaded heat pipes, Journal of Heat Transfer, Vol. 112, pp. 78-83.
8. Park, Y. S., Jung, K. T. and Suh, J. S., 2003, Influence of heat load and operation temperature on the thermal performance of a water-copper variable conductance heat pipe with screen mesh wick, Proceedings of the KSME 2003, Fall Annual Meeting, pp. 9-14.